

## Quantum tunneling and relaxation in $\text{Mn}_{12}$ -acetate studied by magnetic spectroscopy

M. Dressel,<sup>1</sup> B. Gorshunov,<sup>1,2</sup> K. Rajagopal,<sup>1</sup> S. Vongtragool,<sup>1</sup> and A. A. Mukhin<sup>1,2</sup>

<sup>1</sup>Physikalisches Institut, Universität Stuttgart, Pfaffenwaldring 57, D-70550 Stuttgart, Germany

<sup>2</sup>General Physics Institute, Russian Academy of Sciences, 38 Vavilov St., 119991 Moscow, Russia

(Received 2 January 2003; published 25 February 2003)

The spin relaxation in the molecular magnet  $\text{Mn}_{12}\text{ac}$  is investigated by high-frequency magnetic spectroscopy in the frequency domain. By reversing the external magnetic field the intensities of the  $|\pm 10\rangle \rightarrow |\pm 9\rangle$  transitions within the ground multiplet redistribute; below  $T \approx 2$  K resonant quantum tunneling is directly observed as a *tunnel dip* in the absorption spectra of polycrystals. We quantitatively describe our observations by taking into account inhomogeneous line broadening, the time dependence of the level population during the relaxation process, and the resonance behavior of the relaxation rate due to quantum tunneling near the avoided level crossing.

DOI: 10.1103/PhysRevB.67.060405

PACS number(s): 75.50.Xx, 71.70.-d, 75.45.+j, 76.30.-v

In the past years molecular magnets comprising large clusters of coupled magnetic ions have attracted considerable interest as mesoscopic systems which exhibit new properties such as molecular magnetic bistability, macroscopic quantum tunneling of magnetization, quantum phase interference, etc.<sup>1-4</sup> Among them clusters with a high-spin ground state and large anisotropy, such as  $[\text{Mn}_{12}\text{O}_{12}(\text{CH}_3\text{COO})_{16}(\text{H}_2\text{O})_4]2\text{CH}_3\text{COOH} \cdot 4\text{H}_2\text{O}$  (abbreviated as  $\text{Mn}_{12}\text{ac}$ ) are of a paramount interest.

$\text{Mn}_{12}\text{ac}$  cluster can be considered as nanoparticle with an effective magnetic moment of  $20\mu_B$  ( $\mu_B$  is the Bohr magneton), corresponding to a collective spin  $S=10$  of the exchange coupled 12 Mn ions within the molecule. Due to the strong anisotropy, the magnetic moment freezes along one of the two easy directions at low temperatures. This is governed by a crystal field (CF) which splits the ground  $S=10$  multiplet and provides a quasidoublet structure  $|\pm m\rangle$  of the lowest-energy levels. The energy barrier  $\Delta E \approx 60$  K between the two lowest-lying states  $|\pm 10\rangle$  determines the thermally activated relaxation of the magnetization in  $\text{Mn}_{12}\text{ac}$ .<sup>3,4</sup> Below a blocking temperature of about 3-K resonant quantum tunneling was discovered in the form of peaks in the relaxation rate and steps in the hysteresis loops at regular intervals of magnetic field corresponding to a coincidence of the CF energy levels.<sup>1,2</sup> Since the rate of the tunneling for a ground state is small in  $\text{Mn}_{12}\text{ac}$ , the tunneling occurs via appropriate thermally excited CF states for temperatures above approximately 2 K resulting in a shortcut at the top of the barrier which accelerates the relaxation; at even lower temperatures pure quantum tunneling dominates.<sup>3,4</sup>

Various spectroscopic investigations were applied to  $\text{Mn}_{12}\text{ac}$ , including electron-spin resonance (ESR)<sup>5,6</sup> and inelastic neutron scattering.<sup>7</sup> In particular, a new type of high-frequency ESR method based on a quasi-optical spectroscopy<sup>8</sup> made it possible to directly observe the CF transitions in an equilibrium state and to study in details their characteristics, including the line shapes.<sup>9</sup> In this paper we report on the high-frequency magnetic spectroscopy of *non-equilibrium* phenomena in  $\text{Mn}_{12}\text{ac}$  which allows to directly and independently determine the full set of magnetic characteristics.

$\text{Mn}_{12}\text{ac}$  was pressed into a pellet with a thickness of 1.39

mm and a diameter of 10 mm. The high-frequency ESR experiments were performed by means of a quasi-optical coherent-source technique.<sup>10</sup> The transmission spectra  $\text{Tr}(\nu)$  of the pellet were measured with a linearly polarized radiation (its magnetic field denoted as  $\mathbf{h}$ ), in the frequency range  $\nu = 8-12 \text{ cm}^{-1}$  at temperatures down to 1.8 K and in an external magnetic field  $\mathbf{H}$  up to 8 T applied perpendicular to the radiation  $\mathbf{k}$  vector (Voigt geometry). One frequency scan over the full range takes about 20 sec.

Examples of the equilibrium  $\text{Tr}(\nu)$  spectra are shown in Fig. 1(a). The absorption line at  $\nu_0 = 10 \text{ cm}^{-1}$  corresponds to the  $|\pm 10\rangle \rightarrow |\pm 9\rangle$  CF transitions at  $\mathbf{H}=0$ . It shifts to higher frequency  $\nu_H(H) \approx \nu_0 + \gamma|H_z|$  ( $\gamma = g\mu_B/h$ ,  $H_z = H \cos \theta_H$ ,  $\theta_H$  is the angle between  $\mathbf{H}$  and the easy  $C_4$   $z$  axis,  $g \approx 2$ ) and changes its shape with increasing  $\mathbf{H}$ , due to the inhomogeneous splitting of the degenerate  $|\pm 10\rangle$  and  $|\pm 9\rangle$  states in the polycrystalline  $\text{Mn}_{12}\text{ac}$ .

To study *metastable* states of  $\text{Mn}_{12}\text{ac}$  we investigated the time dependence of the  $\text{Tr}(\nu)$  spectra. Applying an external field  $H = +0.45$  T shifts the absorption line to the position  $\nu_H > \nu_0$  [Fig. 1(b)]; we then reverse the field (in about a minute), which shifts the line to the position  $\nu_L \approx \nu_0 - \gamma|H_z| < \nu_0$ . Starting from this point ( $t=0$ ) the intensity of the  $\nu_L$  mode decreases with time while that of the  $\nu_H$  mode recovers correspondingly.

The energy levels of  $\text{Mn}_{12}\text{ac}$  are given by the effective Hamiltonian<sup>5-8</sup>

$$H_{\text{eff}} = DS_z^2 + BS_z^4 + C(S_+^4 + S_-^4)/2 - g\mu_B \mathbf{S} \cdot \mathbf{H}, \quad (1)$$

where  $\mathbf{S}$  is the effective spin of the ground  $S=10$  multiplet, and  $D$ ,  $B$ , and  $C$  are the CF parameters. At small fields the low-energy levels are determined mainly by  $H_z$ :  $E_m = Dm^2 + Bm^4 - g\mu_B H_z m$ ,  $m = 0, \pm 1, \dots, \pm 10$  [inset of Fig. 1(b)]. At low enough temperatures for  $H_z > 0$ , only the  $|+10\rangle$  quantum state is populated and we observe only one magnetic dipole transition  $|+10\rangle \rightarrow |+9\rangle$ . After reversing the field ( $H_z < 0$ ) the state  $|+10\rangle$  becomes metastable and its population relaxes to the new ground state  $|-10\rangle$ ; the intensity of the transition  $|+10\rangle \rightarrow |+9\rangle$  (at  $\nu_L < \nu_0$ ) decreases while that for the transition  $|-10\rangle \rightarrow |-9\rangle$  (at  $\nu_H > \nu_0$ ) grows [Fig. 1(b)]. For our polycrystalline nonoriented sample, a random

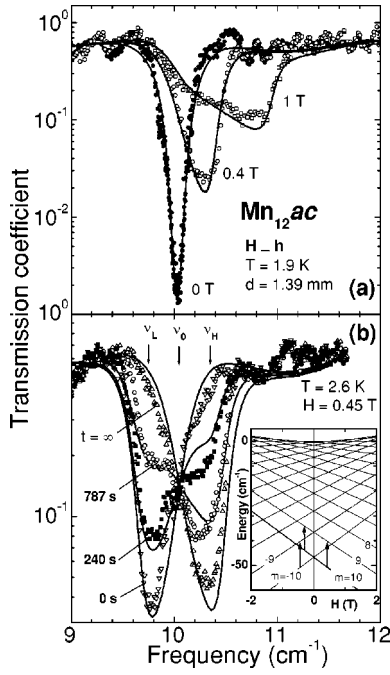


FIG. 1. Transmission spectra of polycrystalline 1.39-mm thick pellet of  $\text{Mn}_{12}\text{ac}2$  measured in an external magnetic field  $\mathbf{H} \parallel \mathbf{h} \perp \mathbf{k}$ . (a) Shift of the absorption line with increasing magnetic field. The solid lines represent the Lorentzian fits with the distribution of the crystallites orientation taken into account. (b) Time evolution of the absorption line after the magnetic field is reversed from  $+0.45$  T to  $-0.45$  T. The lines represent the transmission for the calculated angular distribution of the relaxation time  $\tau(\cos \theta_H)$  exhibit in Fig. 3. The arrows indicate the positions of line at  $\mathbf{H}=0, \pm 0.45$  T. Inset, the energy levels of a  $\text{Mn}_{12}\text{ac}$  single crystal for a magnetic field  $\mathbf{H} \parallel \mathbf{C}_4$ ; the arrows show the  $|\pm 10\rangle \rightarrow |\pm 9\rangle$  transitions before and after the field inversion.

orientation of the easy axis results in the population of both  $|+10\rangle$  and  $|-10\rangle$  CF states and in an inhomogeneous broadening of the corresponding transitions by the applied field.

New features in the relaxation behavior develop at lower temperatures,  $T \leq 2$  K, as shown in Fig. 2. The relaxation occurs *inhomogeneously*; i.e., it has a faster rate near a particular frequency  $\nu_{-}^{(1)} = 9.57 \text{ cm}^{-1}$  where a peak in the  $\text{Tr}(\rho^{(1)})$  spectrum appears accompanied by a minimum at  $\nu_{+}^{(1)} = 10.47 \text{ cm}^{-1}$ . Exhibiting similar fingerprints as the spectral hole burning in dielectrics,<sup>11</sup> this *tunnel dip* in the absorption spectra is due to the azimuthal magnetization hole in those crystallites whose orientation relative to  $\mathbf{H}$  satisfies the level crossing condition  $h\nu_{\pm}^{(1)}(m) = h\nu_0 \pm g\mu_B H_z^{\text{cross}} = h\nu_0 \pm [-D - B(m^2 + (m-1)^2)]$  (resonant quantum tunneling).

For a quantitative description of the observed relaxation, the effective magnetic permeability is calculated using (a) the nonequilibrium populations of the low CF states  $|\pm 10\rangle$  and their evolution (relaxation) with time and (b) the inhomogeneous broadening of the CF transitions in the magnetic field due to the random orientation of the crystallites. First, we analyze a behavior for a single crystallite. Considering only two  $|\pm 10\rangle \rightarrow |\pm 9\rangle$  CF transitions and introducing a nonequilibrium normalized populations  $\rho_m(t)$ , we generalize the ordinary equilibrium permeability<sup>8</sup> and obtain its transverse components,

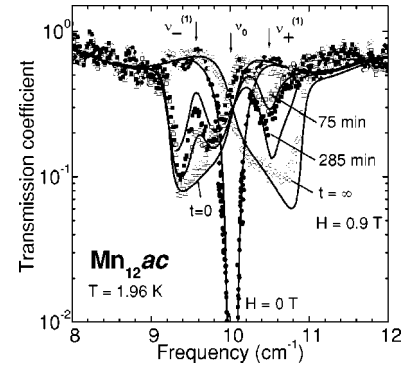


FIG. 2. Time evolution of the transmission spectra at  $T = 1.96$  K after the magnetic field ( $\mathbf{H} \parallel \mathbf{h} \perp \mathbf{k}$ ) is reversed from  $+0.9$  T to  $-0.9$  T. The narrow absorption dip within the broad feature is due to resonant quantum tunneling between pairs of coinciding energy levels. The lines correspond to the transmission spectra for calculated distribution of the relaxation time  $\tau(\cos \theta_H)$  shown in Fig. 3. Also shown is the zero-field absorption line.

$$\mu_{xx,yy}(\nu, t) \equiv \mu_{\perp}(\nu, t) = 1 + \Delta\mu^{+}(\nu, t) + \Delta\mu^{-}(\nu, t), \quad (2a)$$

$$\mu_{xy,yx}(\nu, t) \equiv \pm i\mu_a(\nu, t) = \pm i[\Delta\mu^{+}(\nu, t) - \Delta\mu^{-}(\nu, t)], \quad (2b)$$

where

$$\Delta\mu^{\pm}(\nu, t) = \Delta\mu_0 \left[ \frac{\nu_0}{\nu_{\pm}} (\rho_{\pm 10} - \rho_{\pm 9}) R^{\pm}(\nu) \right]. \quad (3)$$

are the contributions of the  $|\pm 10\rangle \rightarrow |\pm 9\rangle$  CF transitions to the permeability with its static value at  $T=0, H=0$  being  $\Delta\mu_0$ ; a Lorentzian line shape  $R^{\pm}(\nu)$  is assumed for simplicity;  $h\nu_{\pm} = E_{\pm 9} - E_{\pm 10} = h\nu_0 \pm g\mu_B H_z$ . The equilibrium state is given by  $\rho_m(t \rightarrow \infty) = \rho_m^{\infty} = \exp\{-\beta E_m\}/Z$  with  $Z = \sum \exp\{-\beta E_m\}$ ,  $\beta = 1/k_B T$ , and  $\sum \rho_m(t) = 1$ .

In the thermally assisted regime, the relaxation of the populations  $\rho_m(t)$  takes place via excited states and is determined by the complex master equation for the populations of all CF states.<sup>12-15</sup> It can be reduced to the simple relaxation equation  $\Delta\dot{\rho} = -(\Delta\rho - \Delta\rho^{\infty})/\tau$  for  $\Delta\rho = \rho_{+10} - \rho_{-10}$ , where  $\Delta\rho^{\infty} = \rho_{+10}^{\infty} - \rho_{-10}^{\infty}$  is the difference of the equilibrium population after the field is reversed. The solution  $\Delta\rho(t) = \Delta\rho^{\infty}[1 - 2\exp\{-t/\tau\}]$  for the initial condition  $\Delta\rho(0) = \Delta\rho^0 = -\Delta\rho^{\infty}$  leads to the population differences

$$\Delta\rho_{\pm}(t) \equiv \rho_{\pm 10} - \rho_{\pm 9} = \Delta\rho_{\pm}^{\infty} + (\Delta\rho_{\pm}^0 - \Delta\rho_{\pm}^{\infty})e^{-t/\tau}, \quad (4)$$

which enter Eq. (2); here  $\Delta\rho_{\pm}^{\infty} = Z^{-1}[\exp\{-\beta E_{\pm 10}\} - \exp\{-\beta E_{\pm 9}\}]$  and  $\Delta\rho_{\pm}^0 = [1 \mp \Delta\rho^{\infty}(1 + \exp\{-\beta h\nu_{\pm}\})](1 - \exp\{-\beta h\nu_{\pm}\}) / (2 + \exp\{-\beta h\nu_{+}\} + \exp\{-\beta h\nu_{-}\})$ , where all quantities refer to the reversed field. The derivation assumes thermal equilibrium between  $|\pm 10\rangle$  and  $|\pm 9\rangle$  states due to fast relaxation via phonons, implying  $\rho_{\pm 9} = \rho_{\pm 10} \times \exp\{-\beta h\nu_{\pm}\}$ . For low temperatures ( $\beta h\nu_{\pm} \gg 1$ ),  $\rho_{\pm 9}$  is negligible and Eq. (4) simplifies to  $\Delta\rho_{\pm}(t) \approx \rho_{\pm 10}(t) \approx \rho_{\pm 10}^{\infty} + (\rho_{\pm 10}^0 - \rho_{\pm 10}^{\infty})\exp\{-t/\tau\}$ .

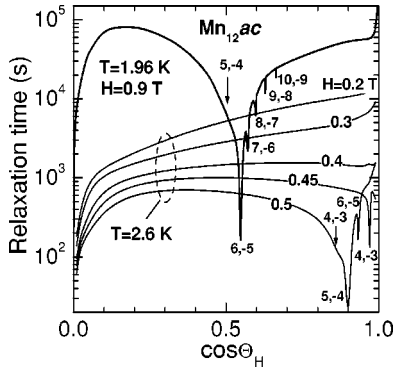


FIG. 3. Calculated distribution of the phonon-assisted spin-tunneling relaxation time  $\tau(\cos\theta_H)$  as a function of the angle between the magnetic field  $\mathbf{H}$  and the  $C_4$  axis of the crystallites at  $T = 2.6$  K and  $T = 1.96$  K for certain values of the applied magnetic field. The numbers at the resonance minima indicate pairs of tunneling CF states.

All previous consideration refers to a single crystal. For polycrystalline samples we have to take into account the inhomogeneous broadening of the lines due to different splittings of the doublets. By averaging the permeability [Eq. (2)] of the crystallites with respect to their orientations, we obtain the effective permeability  $\hat{\mu}^{\text{eff}}(\nu, t)$  with the nonzero components  $\mu_{xx,yy}^{\text{eff}}(\nu, t) = \langle \mu_{\perp}(\nu, t)(1 + \cos^2\theta_H) \rangle / 2$ ,  $\mu_{xy,yx}^{\text{eff}}(\nu, t) = \pm i \langle \mu_a(\nu, t) \cos\theta_H \rangle$ , and  $\mu_{zz}^{\text{eff}}(\nu, t) = \langle \mu_{\perp}(\nu, t) \sin^2\theta_H \rangle$  for the  $\mathbf{H}$  oriented along the  $z$  axis. Using  $\hat{\mu}^{\text{eff}}(\nu, t)$  and the Fresnel formulas for the transmission coefficient<sup>17</sup> we fit the zero-field spectrum and obtain  $\nu_0 = 10.02 \text{ cm}^{-1}$ ,  $\Gamma = 0.18 \text{ cm}^{-1}$ , and  $\Delta\mu_0 = 0.0107$ , in accordance with our previous results.<sup>8</sup> These parameters also describe the spectra in the magnetic field<sup>18</sup> in all details, including the dramatic changes of the line shape [Fig. 1(a)].

The relaxation phenomena observed in our  $\text{Tr}(\nu)$  spectra at various temperatures can be self-consistently described using the theory of the magnetization relaxation in  $\text{Mn}_{12}\text{ac}$ <sup>12-16</sup> based on phonon-assisted spin tunneling induced by fourth-order CF and transverse magnetic field. To determine the relaxation rate  $\tau(T, H, \cos\theta_H)$ , we numerically diagonalize the master equation for the density matrix  $\dot{\rho} = W\rho$  in the space of the ground  $S = 10$  multiplet, following the procedure suggested by Ref. 15. For our calculations we use the CF parameters of Eq. (1),  $D = -0.389 \text{ cm}^{-1}$ ,  $B = -7.65 \times 10^{-4} \text{ cm}^{-1}$ ,  $|C| = 5.0 \times 10^{-5} \text{ cm}^{-1}$  from Refs. 6-8 and parameters of the spin-phonon interaction determined via the main CF term  $DS_z^2$ .<sup>12,14,15</sup>

In Fig. 3 the angular dependence of the relaxation time is plotted for two different temperatures and fields used in our experiments [Figs. 1(b) and 2]. The relaxation goes fastest for  $\cos\theta_H = 0$ , because the energy levels on both sides of the barrier coincide; a situation, however, not observed in Voigt geometry. For fields exceeding the value of the first level crossing ( $\sim 0.44$  T), additional resonance minima arise with a fine structure related to the slightly different resonance conditions for various exciting levels due to the fourth-order CF contribution  $B$ . As an example, Fig. 1(b) shows the relaxation observed in the  $\text{Tr}(\nu)$  spectra at  $H = 0.45$  T and  $T$

$= 2.6$  K, which are well described by our model. We note that a weak resonance near  $\cos\theta_H = 0.97$  due to avoided level crossing of the CF states  $m = 4, -3$  (or  $m = 3, -4$ ) does not exhibit in the spectra due to the averaging in the polycrystalline sample. The relaxation rate strongly increases with magnetic field, because the effective barrier decreases with both (longitudinal and transverse) components;<sup>3</sup> there are also significant contributions from the tunneling processes which are enhanced, because the tunneling splitting increases with the transverse field.<sup>19</sup>

These resonance effects are best seen at low temperatures, when the thermal relaxation over a barrier is suppressed. Figure 3 shows a set of resonances in the relaxation rate at  $T = 1.96$  K which correspond to pairs of states with an avoided level crossing. Using this  $\tau(\cos\theta_H)$ , the time evolution of the  $\text{Tr}(\nu)$  spectra is calculated; as seen from Fig. 2 the agreement is excellent. The main contribution to the resonance relaxation comes from the thermally assisted tunneling via  $(5, -4)$ ,  $(6, -5)$ , and in less degree  $(7, -6)$  states (or corresponding states with the opposite signs); they determine the frequency of the burned spectral hole. For these avoided level crossings the resonance line shape is determined by a truncated Lorentzian<sup>14,15</sup> with the effective linewidth determined by the tunneling splitting ( $0.23$ ,  $0.015$ , and  $5.0 \times 10^{-4} \text{ cm}^{-1}$ , respectively), which is much larger than the corresponding phonon linewidth (ranging from  $5 \times 10^{-6}$  to  $3 \times 10^{-4} \text{ cm}^{-1}$ ). The linewidth ( $0.12$ – $0.18 \text{ cm}^{-1}$ ) of the zero-field-resonance absorption  $\nu_0$  exceeds the corresponding phonon linewidths considerably. It is mainly determined by inhomogeneous broadening and thus serves as a measure of the disorder effects,<sup>9</sup> which could originate from CF and  $g$ -factor distributions ( $D$ -strain and  $g$ -strain) and random magnetic dipolar fields as was shown by ESR.<sup>20</sup>

The problem of shape of the tunneling resonance and the effect of inhomogeneous broadening on it are presently the subject of considerable interest and discussions,<sup>3,12-16,20-26</sup> many issues, however, remain open. One of them could be related to the obvious discrepancy between the observed inhomogeneous character of the zero-field modes broadening<sup>9</sup> and Lorentzian shape of the tunneling resonances observed at temperatures  $T \geq 2$  K,<sup>21,23</sup> and described theoretically in the thermally assisted regime.<sup>14</sup> One may expect that a large inhomogeneous broadening of the levels (i.e., larger than the tunneling splitting) reduces the tunneling amplitudes and smears of the resonances, resulting in suppression of the relaxation peaks and in change of their Lorentzian shape.<sup>15</sup> Suggesting that the main contribution to the line broadening comes from the CF dispersion and assuming its Gaussian distribution,<sup>20</sup> we can evaluate the dispersion  $\delta D = 0.004 \text{ cm}^{-1}$  of the main quadratic term  $D$  in Hamiltonian (1).<sup>27</sup> This yields a smearing of the tunneling level differences  $\delta(E_m - E_{-m+1}) = \delta D(2m - 1)$ , for instance, of  $0.035$ – $0.05 \text{ cm}^{-1}$  for  $(5, -4)$ ,  $(6, -5)$ , and  $(7, -6)$  states. From a comparison with the calculated tunneling splittings, we conclude that the inhomogeneous level broadening does not effect the main resonance  $(5, -4)$ , smears the resonance  $(6, -5)$ , but suppresses the resonance  $(7, -6)$  and higher order resonances. A numerical simulation including an additional averaging with respect to the CF distribution confirms

this conclusion. Thus, if the tunneling splitting is sufficiently large for states contributing to the thermally assisted tunneling, the line shape of the corresponding resonance remains Lorentzian.

In summary, we utilized an optical method of high-frequency magnetic spectroscopy to study the relaxation phenomena in  $\text{Mn}_{12}\text{ac}$  clusters, including the resonance quantum tunneling along with the CF transitions and their line shapes and linewidths. At elevated temperatures only frequency-homogenous relaxation due to mainly thermal activation is observed, whereas for  $T \lesssim 2$  K the thermal relax-

ation is significantly suppressed and resonant quantum tunneling dominates; in this range we observe the *tunnel dip* in the absorption spectra. We have developed a microscopic model which allows to quantitatively describe all observed effects, taking into account the orientational distribution of the relaxation time and to determine the most effective relaxation channels and to estimate the effect of CF inhomogeneity on the resonant tunneling.

We thank Prof. N. Karl for synthesizing the  $\text{Mn}_{12}\text{ac}$ . We acknowledge support from the DFG. This work was supported in part by RFBR (Grant No. 02-02-16597).

- 
- <sup>1</sup>D. Gatteschi *et al.*, *Science* **265**, 1054 (1994).  
<sup>2</sup>J.R. Friedman *et al.*, *Phys. Rev. Lett.* **76**, 3830 (1996); L. Thomas *et al.*, *Nature (London)* **383**, 145 (1996); J.M. Hernandez *et al.*, *Europhys. Lett.* **35**, 301 (1996).  
<sup>3</sup>B. Barbara *et al.*, *J. Magn. Magn. Mater.* **200**, 167 (1999).  
<sup>4</sup>F. Lioni *et al.*, *J. Appl. Phys.* **81**, 4608 (1997).  
<sup>5</sup>S. Hill *et al.*, *Phys. Rev. Lett.* **80**, 2453 (1998); J.A.A.J. Perenboom *et al.*, *Phys. Rev. B* **58**, 330 (1998).  
<sup>6</sup>A.L. Barra *et al.*, *Phys. Rev. B* **56**, 8192 (1997).  
<sup>7</sup>M. Hennion *et al.*, *Phys. Rev. B* **56**, 8819 (1997); I. Mirebeau *et al.*, *Phys. Rev. Lett.* **83**, 628 (1999).  
<sup>8</sup>A.A. Mukhin *et al.*, *Europhys. Lett.* **44**, 778 (1998).  
<sup>9</sup>A.A. Mukhin *et al.*, *Phys. Rev. B* **63**, 214411 (2001).  
<sup>10</sup>A.A. Volkov *et al.*, *Infrared Phys.* **25**, 369 (1985).  
<sup>11</sup>In our case no pump laser saturates the absorption, but a faster second relaxation channel becomes effective.  
<sup>12</sup>D.A. Garanin *et al.*, *Phys. Rev. B* **56**, 11 102 (1997).  
<sup>13</sup>A. Fort *et al.*, *Phys. Rev. Lett.* **80**, 612 (1998).  
<sup>14</sup>M.N. Leuenberger and D. Loss, *Phys. Rev. B* **61**, 1286 (2000).  
<sup>15</sup>T. Pohjola and H. Schoeller, *Phys. Rev. B* **62**, 15 026 (2000).  
<sup>16</sup>F. Luis *et al.*, *Phys. Rev. B* **57**, 505 (1998).  
<sup>17</sup>M. Dressel and G. Grüner, *Electrodynamics of Solids* (Cambridge University Press, Cambridge, 2002).  
<sup>18</sup>Reversing the field, we observe a weak asymmetry of the spectra with respect to the zero-field line position  $\nu_0$  which indicates a small internal dipolar field  $\lambda M \approx 0.04\text{--}0.05$  T; we have included it in our calculations.  
<sup>19</sup>At low temperatures, we observe a much faster relaxation as compared to previous data (Refs. 2,5), because in polycrystalline samples a noticeable transverse component of the magnetic field leads to an increase of the tunneling splitting, and relaxation rate. At higher temperatures the tunneling occurs via excited states with a higher initial tunneling splitting and the effect of the transverse magnetic field diminishes; hence the different data coverage.  
<sup>20</sup>K. Park *et al.*, *Phys. Rev. B* **65**, 014426 (2002); S. Hill *et al. ibid.* **65**, 224410 (2002).  
<sup>21</sup>J.R. Friedman *et al.*, *Phys. Rev. B* **58**, R14 729 (1998).  
<sup>22</sup>N.V. Prokof'ev *et al.*, *Phys. Rev. Lett.* **80**, 5794 (1998).  
<sup>23</sup>W. Wernsdorfer *et al.*, *Europhys. Lett.* **47**, 254 (1999).  
<sup>24</sup>E. Chudnovsky *et al.*, *Phys. Rev. Lett.* **87**, 187203 (2001); D.A. Garanin *et al.*, *Phys. Rev. B* **65**, 094423 (2002).  
<sup>25</sup>R. Amigo *et al.*, *Phys. Rev. B* **65**, 172403 (2002).  
<sup>26</sup>A. Cornia *et al.*, *Phys. Rev. Lett.* **89**, 257201 (2002).  
<sup>27</sup>Imperfections of the crystal, such as dislocations or different isomers, can also promote spin tunneling by inducing a transverse CF (Refs. 24); this was recently observed by ESR in especially prepared  $\text{Mn}_{12}\text{ac}$  samples (Refs. 25,26).